

CTRL Your Shift: Clustered Transfer Residual Learning for Many Small Datasets

Gauri Jain¹, Dominik Rothenhäusler², Kirk Bansak³, Elisabeth Paulson¹

¹Harvard University

²Stanford University

³University of California, Berkeley

Abstract

Machine learning (ML) tasks often utilize large-scale data that is drawn from several distinct sources, such as different locations, treatment arms, or groups. In such settings, practitioners often desire predictions that not only exhibit good overall accuracy, but also remain reliable within each source and preserve the differences that matter across sources. For instance, several asylum and refugee resettlement programs now use ML-based employment predictions to guide where newly arriving families are placed within a host country, which requires generating informative and differentiated predictions for many and often small source locations. However, this task is made challenging by several common characteristics of the data in these settings: the presence of numerous distinct data sources, distributional shifts between them, and substantial variation in sample sizes across sources. This paper introduces Clustered Transfer Residual Learning (CTRL), a meta-learning method that combines the strengths of cross-domain residual learning and adaptive pooling/clustering in order to simultaneously improve overall accuracy and preserve source-level heterogeneity. We provide theoretical results that clarify how our objective navigates the trade-off between data quantity and data quality. We evaluate CTRL alongside other state-of-the-art benchmarks on 5 large-scale datasets. This includes a dataset from the national asylum program in Switzerland, where the algorithmic geographic assignment of asylum seekers is currently being piloted. CTRL consistently outperforms the benchmarks across several key metrics and when using a range of different base learners.

Introduction

Many machine learning (ML) tasks draw data from several distinct sources. A source can be a physical site, a time period, a treatment arm, or any other index that partitions the data. Sources may appear as a categorical feature inside one large data set (e.g. hospital ID, month of year, medical treatment arm), or each source may contribute its own smaller data set collected under local conditions. In any of these settings, practitioners may desire more than predictive accuracy from an ML model: predictions should remain reliable within every source and preserve the differences that matter across sources, so that predictions remain credible for downstream ranking, assignment, and recommendation tasks.

As a concrete example, several asylum and refugee resettlement programs now use ML-based employment predictions

to guide where newly arriving families are placed within a host country (Bansak and Paulson 2024; Ahani et al. 2021). In this setting, the relevant sources are *locations*, and we will use that terminology going forward. Each candidate location (e.g. city, region, state) differs in labor-market conditions, support infrastructure, and demographic composition, all of which influence employment outcomes. Accurate and *location-specific* predictions therefore matter for generating more informed recommendations, clearer communication with local partners, and improved assignment policies.

Building models that have both high predictive accuracy *and* differentiate between locations is difficult for two main reasons. First, locations often vary widely in terms of size. In asylum and refugee programs, geographic quotas (or historical arrival patterns) allocate families unevenly across locations, producing training data sets that range from a handful to many thousands of rows. Small locations inevitably suffer higher estimation error. Second, covariate and outcome distributions differ across locations. Thus, naively pooling all data (henceforth, *global models*) can blur these distribution shifts, while training separate models (henceforth, *local models*) ignores valuable shared structure.

These problem features and challenges hint at two possible adaptive meta-learning strategies that have become increasingly prominent in recent years. However, there are some notable potential tradeoffs between the two strategies.

First, a number of procedures proposed in recent research leverage cross-domain residual learning as a way of tailoring ML models towards specific target data sets or data sources (e.g. Long et al. 2016; Khan and Bremond 2019; Künzel et al. 2019). This aligns with our prioritization of informative location-specific predictions. However, a common weakness of residual learning procedures is that they can often be unreliable for target data sets that are too small. In settings such as ours, the possibility of many small locations potentially limits the effectiveness of residual learning.

Second, other recent research has highlighted the value of adaptive pooling/clustering for handling a collection of data sets or data sources (e.g. Shen, Raji, and Chen 2024; Jeong and Rothenhäusler 2024; Huang and Wang 2025). The advantage offered by this strategy is in borrowing strength across locations, bolstering predictive performance even for small locations. When pooling is performed with *overall* accuracy in mind, however, such an approach may fail to capture het-

erogeneity specific to different locations. Accounting for this type of heterogeneity is vital in a setting such as ours, where differentiated predictions across locations are foundational for guiding downstream tasks.

In this paper, we propose a meta-learning approach that seeks to leverage the strengths of both strategies by navigating their tradeoffs in a principled fashion. First, we anchor our approach by establishing a baseline procedure—which we refer to as *transfer residual learning (TRL)*—that trains a global model on the pooled dataset, and then fine-tunes location-specific residual models to capture systematic deviations. This two-stage baseline approach leverages the pooled dataset for generalization while allowing location-level corrections. However, performance is limited by location size: small locations may still suffer from high variance in their fine-tuning step. To address this limitation, we propose *Clustered Transfer Residual Learning (CTRL)*, a new meta-learning algorithm that identifies clusters of locations that improve a target location’s fine-tuning step (See Figure 1). By adaptively clustering locations, CTRL automatically adapts to location similarity and data availability. When no meaningful cluster exists for a location, the method defaults to baseline transfer residual learning, and when location membership carries little predictive information, it reverts to a global model. This adaptive design enables CTRL to achieve more accurate predictions, particularly for small locations, while retaining predictive differentiation. Furthermore, CTRL is agnostic to the base learner used for model building (e.g. linear regression, random forest, etc.).

We evaluate CTRL, baseline transfer residual learning, and additional state-of-the-art benchmarks on 5 large-scale datasets—including a dataset from the national asylum program in Switzerland, where the algorithmic geographic assignment of asylum seekers is currently being piloted (Bansak and Paulson 2024). For three datasets, we evaluate three metrics: (1) overall mean squared error (MSE), (2) MSE among small locations, and (3) rank-weighted average (RWA). Inspired by Yadlowsky et al. (2025), RWA captures how well each location can identify top-performing individuals, serving as a proxy for a model’s ability to perform well on downstream tasks such as ranking, assignment, and allocation. For the remaining two datasets, we report only the MSE metrics, as they do not support a meaningful notion of ranking. Our results show that CTRL consistently outperforms the benchmarks in all three metrics. This strong performance demonstrates the value of considering CTRL for deployment in algorithmic asylum and refugee resettlement efforts, among other possible settings.

Contributions

Our main contributions are as follows:

- We introduce *Clustered Transfer Residual Learning (CTRL)*, a meta-learning algorithm for the many-locations prediction problem that addresses both distribution shift and data scarcity within individual domains. We provide a theoretical justification for this clustering procedure that reveals tradeoffs between data set size and distribution

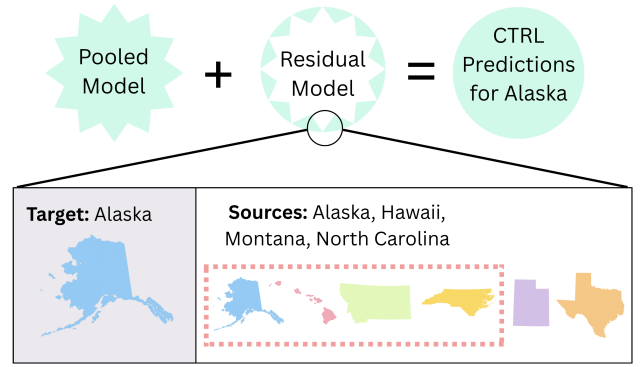


Figure 1: An overview of CTRL on the example task of predicting educational attainment in the state of Alaska. CTRL’s predictions are the sum of (1) predictions from a pooled model using all education data from the the US and (2) predictions from a residual model that clusters location datasets from Alaska, Hawaii, Montana, and North Carolina.

shift. Our code and datasets are publicly available.¹

- We benchmark CTRL against global, local, and residual learning techniques as well as two state-of-the-art meta-learning algorithms. We consistently show improved performance using a range of model architectures, including linear models, decision trees, and ensemble methods. We evaluate all methods on a large asylum seeker dataset from Switzerland, and four additional datasets from various application domains.

Related Work

Fine Tuning and Residual Learning. Our approach leverages a form of model stacking or residual learning, which has a long history in machine learning (Wolpert 1992), and is related to popular approaches such as gradient boosting (Friedman 2001) and fine-tuning (Yosinski et al. 2014). The proposed approach combines a form of residual learning with data-set adaptive pooling, to improve performance for small data sets under distribution shift.

Robust machine learning. Zhang, Huang, and Imai (2024) focus on robustifying measurements of treatment effects by learning heterogeneous treatment predictions that work well across multiple domains. Group distributionally robust optimization (Group DRO) (Sagawa et al. 2020) learns a prediction model by optimizing the worst-case group risk. Xie et al. (2023) propose training a small proxy model using Group DRO to select domain weights. In our setting, such approaches would yield the same prediction for every location, thereby undermining the downstream decision task of leveraging location-specific synergies. Simple data-set balancing via re-weighting has been shown to have competitive worst-group accuracy (Idrissi et al. 2022). Just Train Twice (JTT) (Liu et al. 2021) is designed to improve worst-case performance. However, such procedures can exhibit overly conservative performance in terms of average-case MSE.

¹<https://anonymous.4open.science/r/CtrlYourShift-258B/>

Causal Inference. In causal inference, the focus is often on learning the contrast between a treatment and control group, which can be seen as two different distributions. Thus, many heterogeneous treatment effect estimators can be re-framed as cross-domain residual learning strategies. Nie and Wager (2020) provide a loss minimization framework for heterogeneous treatment effect estimation based on Robinson’s decomposition. Our approach is related to Künzel et al. (2019), who combine multiple residual learning models for heterogeneous treatment effect estimation. However, this type of residual learning is not appropriate in the many-data set setting, since it ignores the shared structure across multiple small data sets.

Data set pooling under distribution shift. Given the breadth of work on data pooling, we restrict our discussion to recent developments. In Shen, Raji, and Chen (2024), the authors discuss how aggregating data from many diverse sources can sometimes harm model performance due to distribution shifts—a challenge they term the Data Addition Dilemma. They propose heuristics to guide data selection for improved accuracy and robustness. Our procedure is similar in the sense that we also adaptively add data sets that are “close” to the target in some sense, but we measure the closeness in terms of residual unexplained variance instead of the joint (X, Y) distribution. Ye et al. (2024) use data scaling laws to identify optimal data mixtures; however, the proposed method does not scale to settings with a large number of datasets. Furthermore, Ye et al. (2024) address a different performance–speed tradeoff relevant to large language model training, which differs from the setting considered here.

Data Generation Techniques. Oversampling methods such as SMOTE (Bowyer et al. 2011), data generation techniques like mixup (Zhang et al. 2018) and interpolation-based approaches (Fan and Alvarez-Melis 2023) offer solutions for mitigating class imbalance by artificially augmenting the dataset. However, these approaches are often not viable in real-world deployments due to the potential liabilities associated with generating synthetic data. Additionally, when certain subgroups contain lower-quality or noisier data, such techniques may reduce robustness by amplifying the influence of unreliable samples through oversampling.

Methodology

Preliminaries

We consider a training dataset $\mathcal{D}_{\text{train}} = \{(X_i, M_i, Y_i)\}_{i=1}^{n_{\text{train}}}$ of size n_{train} , where each individual i is associated with a feature vector $X_i \in \mathcal{X}$, a location designation $M_i \in \mathcal{M}$, and a response variable $Y_i \in \mathcal{Y}$. We assume that location designation forms a partition of the training data into $|\mathcal{M}|$ disjoint groups such that each individual belongs to exactly one location. let $\mathcal{D}_{\text{train}}^g = \{(X_i, M_i, Y_i) : M_i = g\}$ be the subset of the data corresponding to location $g \in \mathcal{M}$. For this paper, we set \mathcal{M} to represent locations, but \mathcal{M} could more generally denote any (mutually exclusive and collectively exhaustive) set of data sources, groupings, or partitions.

We aim to learn a predictive model $\hat{f} : \mathcal{X} \times \mathcal{M} \rightarrow \mathcal{Y}$ from the training data, which maps features and location to

predicted outcomes.

In addition to the training data, we consider a test dataset $\mathcal{D}_{\text{test}} = \{(X_i, M_i, Y_i)\}_{i=1}^{n_{\text{test}}}$ consisting of n_{test} individuals, which we use to evaluate the performance \hat{f} .

Residual Learning

Residual learning follows a two-stage meta-learning framework, where each component model may be instantiated with any supervised learning method. We call this model \hat{f}_{TRL} for Transfer Residual Learning because it estimates residuals using a combination of pooled and location-specific data.

In the first stage, we use the entire training dataset to train a base model $\hat{f}_{\text{base}} : \mathcal{X} \times \mathcal{M} \rightarrow \mathcal{Y}$ to predict the outcome Y_i using covariates X_i , and location designation M_i : $\hat{f}_{\text{base}}(X_i, M_i) \approx \mathbb{E}[Y_i | X_i, M_i]$. In the second stage, we refine the base model through residual learning to capture location-specific heterogeneity. For an individual i belonging to location g , we define the residual as: $R_i^g = Y_i - \hat{f}_{\text{base}}(X_i, g)$.

For each location $g \in \mathcal{M}$, we train a residual model $\hat{f}_{\text{residual}}^g : \mathcal{X} \rightarrow \mathbb{R}$ using only individuals with $M_i = g$, aiming to satisfy $\hat{f}_{\text{residual}}^g(X_i) \approx R_i^g$ for all i in location g . The final prediction for individual i in location g is given by

$$\hat{f}_{\text{TRL}}(X_i, g) = \hat{f}_{\text{base}}(X_i, g) + \hat{f}_{\text{residual}}^g(X_i),$$

which combines the global base model with a location-specific correction.

Clustered Transfer Residual Learning

CTRL extends the residual learning framework by replacing location-specific residual models with cluster-specific residual models. Each cluster consists of one or more locations, enabling shared learning across structurally similar or data-sparse subpopulations (see Figure 1 as an example). Let $\mathcal{C}(g) \subseteq \mathcal{M}$ denote the cluster constructed for location g . We define $\hat{f}_{\text{residual}}^{\mathcal{C}(g)}$ as the residual model trained using all training data from locations in $\mathcal{C}(g)$. The final prediction for an individual i in location g is:

$$\hat{f}_{\text{CTRL}}(X_i, g) = \hat{f}_{\text{base}}(X_i, g) + \hat{f}_{\text{residual}}^{\mathcal{C}(g)}(X_i).$$

For each location, searching over all $2^{|\mathcal{M}|}$ possible clusters is computationally infeasible, so we propose a data-driven heuristic for identifying effective clusters. Let $h^g(r | X)$ denote the conditional distribution of residuals $r = Y - \hat{f}_{\text{base}}(X, g)$ for location g . If two locations g_1 and g_2 satisfy $h^{g_1}(r | X = x) = h^{g_2}(r | X = x)$ for all x , then pooling should decrease error, since it does not introduce bias. When h^{g_1} and h^{g_2} differ, pooling their data may help or harm the residual model for location g_1 , depending on the similarity of their distributions and relative sizes. This tradeoff is especially pronounced when one location is much larger.

To construct clusters, we focus on a target location $g \in \mathcal{M}$. We partition the training data into a random 80/20 split, denoted $\mathcal{D}_{\text{train}}^{80}$ and $\mathcal{D}_{\text{train}}^{20}$. On $\mathcal{D}_{\text{train}}^{80}$, we train \hat{f}_{base} and location-specific residual models $\hat{f}_{\text{residual}}^m$ for all locations $m \in \mathcal{M}$. For each individual $i \in \mathcal{D}_{\text{train}}^{g, 20} := \{i \in \mathcal{D}_{\text{train}}^{20} | M_i = g\}$, we

compute $r_{im} = \hat{f}_{\text{residual}}^m(X_i)$ for all $m \in \mathcal{M}$, which represents the predicted residual for individual i if they belonged to location m . Recall that we define the actual residual as $R_i^g = Y_i - \hat{f}_{\text{base}}(X_i, g)$. To find a suitable cluster for location g , we solve the following optimization problem:

$$\begin{aligned} \min_{\mathbf{z}} \quad & \sum_{i=1}^{|\mathcal{D}_{\text{train}}^{m,20}|} (R_i^g - \frac{\sum_{m=1}^{|\mathcal{M}|} z_m r_{im} n_m}{\sum_{m=1}^{|\mathcal{M}|} z_m n_m})^2 \\ \text{s.t.} \quad & \mathbf{z} \in \{0, 1\}^M \quad \forall m \in \{1, \dots, |\mathcal{M}|\} \\ & z_g = 1, \end{aligned} \quad (1)$$

where z_m is a binary decision variable indicating whether location m is included in the cluster for location g , and n_m is the size of location m . We denote the selected cluster as $\mathcal{C}(g) = \{m : z_m^* = 1\}$, where \mathbf{z}_g^* is the optimal solution to Problem 1. The objective seeks to find a weighted combination of residual models that best approximates the actual residuals of location g , giving more weight to location with large sample size. While many current methods for data selection focus on data weighting rather than pooling (Idrissi et al. 2022; Xie et al. 2023; Jeong and Rothenhäusler 2025), we found that many state-of-the-art algorithms perform sub-optimally under re-weighting for real-world data, which we also show with one of our benchmarks (RWG). Thus, we focus on data pooling instead of data weighting.

Problem 1 is nonlinear and nonconvex, but it can be optimally solved using modern mixed-integer programming solvers. Inspired by stabilization procedures in Meinshausen and Bühlmann (2010), we repeat this procedure 250 times with different training splits (see Appendix for all hyperparameter information). This pipeline is summarized in Algorithm 1. As a post-processing step, we also define $\mathbf{w}_g \in [0, 1]^{|\mathcal{M}|}$ which denotes a vector where each entry $w_{g,m}$ represents the fraction of iterations in which $z_{g,m}^* = 1$ when solving Problem 1 for location g . Since solving Problem 1 hundreds of times for each location can be computationally expensive when M is large, we restrict the candidate set to a random subset of locations always including g in each run (denoted by regularization parameter λ).

Algorithm 1: CTRL: Generate Decision Variable

```

1: Input:  $\mathcal{D}_{\text{train}}, \mathcal{D}_{\text{test}}$ , iteration seed  $iter$ ,  $g$ , regularization par  $\lambda$ 
2: Output: Weight vector  $\mathbf{z}_g^*$  for location  $g$ 
3: Split  $\mathcal{D}_{\text{train}}$  into:  $\mathcal{D}_{\text{train}}^{80}$  (80% train),  $\mathcal{D}_{\text{train}}^{20}$  (20% validation)
4: Train  $\hat{f}_{\text{base}}$  on  $\mathcal{D}_{\text{train}}^{80}$ 
5: for each group  $m \in \mathcal{M}$  do
6:   Compute  $R_i^m = Y_i - \hat{f}_{\text{base}}(X_i, m)$  for  $i \in \mathcal{D}_{\text{train}}^{m,80}$ 
7:   Train residual model  $\hat{f}_{\text{residual}}^m$  on  $\mathcal{D}_{\text{train}}^{m,80}$ 
8:   Compute  $r_{im} = \hat{f}_{\text{residual}}^m(X_i)$  for  $i \in \mathcal{D}_{\text{train}}^{g,20}$ 
9: end for
10: Compute  $R_i^g = Y_i - \hat{f}_{\text{base}}(X_i, g)$  for  $i \in \mathcal{D}_{\text{train}}^{g,20}$ 
11: Solve Problem 1 using  $R_i^g$  and  $r_{im}$  to obtain  $\mathbf{z}^*$ 
12: return  $\mathbf{z}_g^*$ 

```

We use Algorithm 2 to construct the final cluster for location g . We begin with $\mathcal{C}(g) = \{g\}$ and iteratively add locations in decreasing order of values in \mathbf{w}_g . We consider

the top ten locations in \mathbf{w}_g . After each addition, we train $\hat{f}_{\text{residual}}^{\mathcal{C}(g)}$ and evaluate its MSE on $\mathcal{D}_{\text{train}}^{g,20}$. We repeat across 250 splits and apply the “1 Standard Error Rule” (Hastie et al. 2004) to determine the optimal cluster for g , $\mathbf{C}^*(g)$. Lastly, we train \hat{f}_{base} on $\mathcal{D}_{\text{train}}$, train $\hat{f}_{\text{residual}}^{\mathbf{C}^*(g)}$ on $\mathcal{D}_{\text{train}}^{\mathbf{C}^*(g)}$, and add them up to model \hat{f}_{CTRL} which we use to evaluate on $\mathcal{D}_{\text{test}}^g$.

Algorithm 2: CTRL: Get Optimal Cluster

```

1: Input:  $\mathcal{D}_{\text{train}}, g$ , fractional decision weights  $\mathbf{w}_g$ 
2: Output: Optimal cluster for location  $g$ 
3: for iter = 1 to 250 do ▷ Perform 250 iterations
4:   Split  $\mathcal{D}_{\text{train}}$  into:  $\mathcal{D}_{\text{train}}^{80}$  (80% train),  $\mathcal{D}_{\text{train}}^{20}$  (20% validation)
5:   Train base model  $\hat{f}_{\text{base}}$  on  $\mathcal{D}_{\text{train}}^{80}$ 
6:   for  $k = 1$  to 10 do ▷ Vary number of locations
7:      $\mathcal{C}_k(g) \leftarrow$  top  $k$  indices of  $\mathbf{w}_g$ 
8:     Train  $\hat{f}_{\text{residual}}^{\mathcal{C}_k(g)}$  from data from  $\mathcal{D}_{\text{train}}^{\mathcal{C}_k(g),80}$ 
9:     Compute predictions  $r_g$  on  $\mathcal{D}_{\text{train}}^{g,20}$ 
10:     $\text{MSE}_g \leftarrow \frac{1}{n_g} \sum_{i \in \mathcal{D}_{\text{test}}^g} (Y_i^g - (\hat{f}_{\text{base}}(X_i, g) + r_{ig}))^2$ 
11:  end for
12: end for
13:  $\forall k = 1$  to 10, compute  $\bar{\text{MSE}}_g^k$  and  $\text{SE}_{\text{MSE},g}^k$  over 250 iterations
14:  $k^{\min} := \arg \min_k \bar{\text{MSE}}_g^k$  ▷ 1 Std Error rule
15:  $\text{MSE}_g^{\text{cutoff}} = \bar{\text{MSE}}_g^{k^{\min}} + \text{SE}_{\text{MSE},g}^{k^{\min}}$ 
16:  $k_g^* := \min_k (\bar{\text{MSE}}_g^{(k)} \leq \text{MSE}_g^{\text{cutoff}})$ 
17: return  $\mathbf{C}^*(g) =$  top  $k_g^*$  locations from  $\mathbf{w}_g$ 

```

Theoretical Results

To theoretically characterize the tradeoff between dataset size and distribution shift in our objective (1), we build on the random distributional shift model (Bansak, Paulson, and Rothenhäusler 2024; Jeong and Rothenhäusler 2024). This is a stylized model that assumes that the likelihood ratio between the source distributions and target distributions is random. In brief, pooling increases the effective sample size but can introduce estimation error due to distributional mismatches between source and target locations. Our results show that the excess risk scales with (1) model complexity, (2) outcome noise, (3) the strength of distributional shift, and (4) the proportion of data drawn from shifted sources.

We will now list the main assumptions underlying a random distribution shift. For simplicity, we consider the target distribution P^g as fixed and we have access to several randomly shifted source distributions $P^m, m = 1, \dots, |\mathcal{M}|$.

Random distribution shift. Let I_1, \dots, I_K be a disjoint partitioning of the sample space $\mathcal{X} \times \mathcal{Y}$, with $P^g((X, Y) \in I_k) = 1/K$. We assume that as $K \rightarrow \infty$, the partitioning approximates all square integrable functions², i.e. $\lim_{K \rightarrow \infty} E_g[(f(X, Y) - E[f(X, Y)|I_\bullet])^2] \rightarrow 0$ for all $f(X, Y) \in L^2(P^g)$. For $(x, y) \in I_k$ let

$$P^m(x, y) = \frac{W_k^m}{\frac{1}{K} \sum_{k'=1}^K W_{k'}^m} P^g(x, y),$$

²This can be achieved by a standard partitioning approach. For instance, if Y is a continuous random variable, endpoints of intervals I_k can be defined via the $\frac{k-1}{K}$ -th and $\frac{k}{K}$ -th quantiles of Y .

for some set of positive random weights W_k^m . We assume that the vectors (W_k^1, \dots, W_k^M) are i.i.d. across $k = 1, \dots, K$. We draw n_m many (X, Y) observations from P^m for $m = 1, \dots, |\mathcal{M}|$. That is, conditional on P^m , the observations from location m are independent.

We consider the simplified setting where each model computes a simple average of outcomes within a fixed leaf $L \in \mathcal{L}$, where \mathcal{L} is a partition of \mathcal{X} (e.g., as in regression trees with fixed splits). In practice, the fixed leaf assumption can be satisfied via sample splitting: tree structure is learned on one half of the data and leaf averages are estimated on the other, ensuring the splits are independent of the noise. Let $\mathcal{C} \subseteq \mathcal{M}$ denote a fixed cluster and define the excess risk

$$\mathcal{E}_g = E_g \left[\left(R^g - \frac{\sum_{m=1}^{|\mathcal{M}|} z_m r_m n_m}{\sum_{m=1}^{|\mathcal{M}|} z_m n_m} \right)^2 \right] - E_g[(Y - E_g[Y|\mathcal{L}])^2].$$

This corresponds to the difference of the expected value of our objective (1) and the MSE of prediction $E_g[Y|\mathcal{L}]$, which is the optimal prediction for a tree with splits \mathcal{L} . The proof of the following result can be found in the Appendix.

Proposition 1 (Excess risk under distribution shift). *Let $K, n_m \rightarrow \infty$ with $K/n_m \rightarrow c_m \in (0, \infty)$. Write $n_m^* = \lim n_m / \sum_{m'} n_{m'}$. Let $\text{Var}_g(Y) \in (0, \infty)$ and $P_g(X \in L) > 0$ for all $L \in \mathcal{L}$. Then, $K \cdot \mathcal{E}_g$ converges to a non-degenerate random variable with mean*

$$\left(\beta(\mathcal{C})^\top \Sigma^W \beta(\mathcal{C}) + \sum_m \beta(\mathcal{C})_m^2 c_m \right) \cdot \sum_{L \in \mathcal{L}} \text{Var}_g(Y | X \in L),$$

where $\beta(\mathcal{C})_m = \frac{1_{m \in \mathcal{C}} n_m^*}{\sum_{m' \in \mathcal{C}} n_{m'}^*}$.

For simplicity, let us consider the case where we have some data from the target P^g and some data from another location P^m and define $\sigma_{\text{avg}}^2 = \frac{1}{L} \sum_{L \in \mathcal{L}} \text{Var}_g(Y|X \in L)$ as the average noise (over the leaves). In that case, the expected excess risk of training only on g 's data is $\frac{1}{n_g} \cdot |\mathcal{L}| \cdot \sigma_{\text{avg}}^2$. If we train on data from P^g and P^m , the expected excess risk is

$$\left(\underbrace{\frac{\Sigma_{mm}^W}{K}}_{\text{shift strength}} \cdot \underbrace{\frac{n_m^2}{(n_m + n_g)^2}}_{\text{prop. shifted data}} + \underbrace{\frac{1}{n_g + n_m}}_{\text{pooled sam. size}} \right) \cdot \underbrace{|\mathcal{L}|}_{\# \text{ params}} \cdot \underbrace{\sigma_{\text{avg}}^2}_{\text{noise}}$$

We can think about $\frac{\Sigma_{mm}^W}{K}$ as the strength of distribution shift. If n_m is much larger than n_g , then the distribution shift hurts performance more since the data from P^m is a larger share of the total training data. Thus, there is a tradeoff between data quantity and data quality (measured via the strength of distribution shift between source m and target g).

Datasets

We evaluate our method on 5 datasets and provide 4 in our codebase (See Appendix for more dataset information).

Synthetic dataset. We generate dataset of 40,000 individuals divided into 50 locations, with location sizes ranging from 40 to 2,000. For each individual, we compute a probability of success using a weighted combination of a global linear

model (30%) and location-specific local linear models (70%). A subset of locations share similar local models to simulate a clustered structure. Binary outcomes are sampled from these probabilities, enabling evaluation on both the prediction and ranking tasks. We provide the script to generate this.

Swiss asylum seekers dataset. This administrative dataset from the Central Migration Information System (ZEMIS) of the Swiss State Secretariat for Migration contains background characteristics, assigned location (of which there are 26), and employment outcomes for adult asylum seekers entering Switzerland who were granted a protected status.³ The dataset comprises individuals who were assigned to a canton between 2018-2022. We use a binary two-year employment outcome as the outcome of interest, encoding whether an individual found *any* employment in their first two years after assignment. This dataset is not publicly available but can be requested from the Swiss State Secretariat for Migration. The study received IRB approval from Harvard University (IRB22-1083).

Education dataset. We use U.S. Census data from 2014 to predict whether individuals over 18 have completed high school – using (Ding et al. 2021) for preprocessing. We select 14 demographic and background variables (e.g., language, disability status, state, country of birth), and use state as the location variable.

Dissecting Bias health dataset. This semi-synthetic health dataset (Obermeyer et al. 2019) includes patient records with binary outcomes marking chronic illness. Each observation includes features like demographics, comorbidities, prior costs, biomarkers, and medications. Instead of geographic locations as the source, we define “source” as combinations of race, age, and gender (e.g. *Black, 20-30 years old, female*).

UK asylum decisions dataset. This dataset⁴ includes asylum applications and resettlement decisions in the United Kingdom, disaggregated by nationality, demographic attributes, and administrative attributes such as time and case details. We define “sources” as nationalities (instead of locations) and predict the likelihood of an individual asylum request being approved by a judge.

Model Evaluation

Metrics

We evaluate models using three key metrics: (1) overall mean squared error (MSE), (2) MSE for small locations (defined as the bottom third by location size), and (3) the average outcome among the top 20% of individuals ranked by each location according to each method, or Rank-Weighted Average (RWA), inspired by Yadlowsky et al. (2025). RWA evaluates whether a model effectively prioritizes individuals who are likely to benefit most from being matched to a given

³Specifically, the data contain asylum seekers who eventually received full protection status specified under the Geneva Convention as well as those whose claim for Geneva protection status was rejected but were awarded subsidiary protection.

⁴<https://www.gov.uk/government/statistical-data-sets/asylum-and-resettlement-datasets>

location. For each location $g \in \mathcal{M}$, we identify the top 20%⁵ of individuals with the highest \hat{Y}_{ig} , where \hat{Y}_{ig} denotes the prediction for individual i at location g . Let S_g be the set of these top-scoring individuals for location g .

$$\text{RWA} = \frac{1}{|\mathcal{A}|} \sum_{i \in \mathcal{A}} Y_i \quad \text{where} \quad \mathcal{A} = \bigcup_{g \in \mathcal{M}'} \{i \in S_g : M_i = g\}$$

The set \mathcal{A} contains individuals who were both in the top 20% for some location g and actually assigned to g in the data. Rather than consider all locations \mathcal{M} , we restrict attention to \mathcal{M}' —the set of locations where $|\{i \in S_g : M_i = g\}| \geq 10$ across all models.

In the Swiss asylum context, the historical assignment procedure satisfies conditional ignorability (i.e. conditional upon the covariates we have access to), and thus the predictions can be interpreted causally. Thus, in this setting RWA approximates the counterfactual outcome if the top 20% of individuals were actually assigned to g .

Benchmarks

We evaluate against several benchmark algorithms and underlying architectures. Following prior work using these datasets (Liu et al. 2023; Bansak, Paulson, and Rothenhäusler 2024), we identify the most consistently high-performing model architectures—namely, tree ensembles. As such, we include results for both Bayesian Additive Regression Trees (BART) and Random Forest (RF), which serve as strong performance benchmarks for our setting. Given the real-world settings in our work, we also report results using interpretable models (linear regression and decision trees) which are often preferred by practitioners in high-stakes contexts (Rudin 2019).

In addition to TRL, global models, and local models as baseline methods, we also include two state-of-the-art methods for learning with imbalanced or heterogeneous-source data: JTT and RWG (Liu et al. 2021; Idrissi et al. 2022). For the RWG benchmark, we assign weights to ensure that each location contributes equally to the model’s objective, so that the loss from a small location is given the same importance as that from a large location. While Group-DRO is another benchmark often used for predictions for datasets with multiple subgroups, it is irrelevant for our use case because it would output the same predictions for each location, which does not address our of differentiating between locations.

Experimental Results

Synthetic Results

We begin by evaluating model performance on a synthetic dataset (Table 1). CTRL consistently outperforms all benchmarks across MSE, small-location MSE, and RWA. Since the data are generated from linear functions at the location level, it is expected that the local regression model performs well

⁵We chose the 20% cutoff for these results to balance identifying top performers while ensuring location-level variation in candidate selection. We provide results for other cutoffs in the appendix and our model still outperforms the others (Appendix: Table 3).

on overall MSE. However, CTRL is the only model achieving overall accuracy comparable to that of the local model. Additionally, the performance gap between CTRL and other methods—including the local model—becomes more pronounced for small location MSE and RWA. This highlights a core limitation of local models: poor performance on small locations. In contrast, CTRL delivers reliable performance overall and for small locations.

Swiss Asylum Seekers and Education Datasets

We next evaluate performance on real-world datasets, beginning with our Swiss data on asylum seekers. As seen in Table 1, CTRL consistently outperforms other models in both overall MSE and RWA. This indicates that CTRL not only delivers the most accurate predictions overall, but also excels at identifying individuals who are the best matches for each location. This is an essential capability for this setting, where resettlement staff—with assistance from an algorithm—determine the geographic placement of asylum seekers.⁶ Importantly, CTRL’s advantage over the global model on RWA suggests that it does more than rank the most “globally employable” individuals highest everywhere. Instead, it captures location-specific heterogeneity, tailoring rankings to the distinctive labor markets and characteristics of each location.

For smaller locations, CTRL’s performance is nearly on par with the best-performing benchmarks, demonstrating that it remains competitive in data-sparse regions. Notably, the RWG benchmark performs well on small-MSE, as expected since it up-weights small-location data. However, this comes at a substantial cost: RWG underperforms on overall MSE and RWA, making it a less favorable choice in practice.

We also report results on an Educational Outcomes dataset to illustrate the robustness of CTRL. While this dataset does not support causal claims—as individuals are not randomly assigned to states—it provides a testbed for generalization. As shown in Table 1, CTRL either achieves or ties for the lowest MSE, and also achieves the best RWA.

Additional Datasets without Locations as Sources

Lastly, we examine datasets where sources are defined not as locations but by demographic characteristics. In such settings, RWA is not an applicable metric, as the source attribute is not assignable. Nevertheless, CTRL remains valuable: even without a downstream task, it consistently performs well in predictive performance on imbalanced datasets. Table 2 reports results on two such datasets: UK asylum decisions and the Dissecting Bias Health dataset. CTRL consistently outperforms other benchmarks in both MSE metrics, underscoring its utility when the primary goal is solely prediction accuracy.

Overall Performance

To compare overall model performance across datasets, we use an average rank metric which is standard for multi-dataset evaluation (Demšar 2006). We exclude the Synthetic dataset since it was constructed specifically for our use case. Figure 2 reports the average rank of each model across all

⁶In this context, the assignment procedure satisfies conditional ignorability, and thus the predictions can be interpreted causally.

Table 1: MSEs and RWA across 3 datasets. Bold indicates best performance. Lower is better MSEs, higher is better for RWA.

Dataset	Model	MSE				Small MSE				RWA			
		Reg	Tree	RF	BART	Reg	Tree	RF	BART	Reg	Tree	RF	BART
Synthetic	JTT	0.209	0.264	0.222	0.244	0.214	0.272	0.227	0.249	0.789	0.604	0.784	0.798
	RWG	0.210	0.246	0.219	0.213	0.214	0.789	0.222	0.215	0.789	0.669	0.759	0.778
	Global	0.209	0.233	0.215	0.197	0.225	0.244	0.229	0.222	0.744	0.686	0.732	0.769
	Local	0.133	0.243	0.191	0.158	0.168	0.260	0.211	0.187	0.930	0.661	0.884	0.907
	TRL	0.138	0.226	0.176	0.153	0.167	0.244	0.200	0.176	0.934	0.726	0.863	0.911
	CTRL	0.134	0.222	0.170	0.147	0.140	0.233	0.183	0.156	0.957	0.745	0.895	0.933
Swiss Asylum Seekers	JTT	0.121	0.202	0.148	0.121	0.117	0.228	0.154	0.117	0.264	0.245	0.243	0.251
	RWG	0.119	0.139	0.112	0.116	0.114	0.137	0.106	0.108	0.270	0.371	0.342	0.309
	Global	0.120	0.123	0.110	0.114	0.119	0.124	0.109	0.112	0.269	0.484	0.376	0.338
	Local	0.121	0.124	0.112	0.119	0.136	0.141	0.126	0.128	0.267	0.370	0.307	0.284
	TRL	0.118	0.121	0.108	0.112	0.121	0.123	0.115	0.113	0.272	0.486	0.377	0.333
	CTRL	0.118	0.121	0.107	0.113	0.121	0.124	0.108	0.113	0.274	0.484	0.390	0.341
Education	JTT	0.159	0.232	0.217	0.207	0.157	0.243	0.212	0.201	0.936	0.893	0.908	0.944
	RWG	0.159	0.169	0.156	0.161	0.155	0.160	0.153	0.154	0.937	0.919	0.940	0.940
	Global	0.153	0.156	0.152	0.151	0.155	0.159	0.153	0.154	0.940	0.913	0.942	0.943
	Local	0.163	0.175	0.166	0.152	0.172	0.184	0.170	0.162	0.898	0.878	0.932	0.940
	TRL	0.152	0.154	0.151	0.150	0.156	0.159	0.153	0.155	0.941	0.926	0.944	0.943
	CTRL	0.151	0.154	0.150	0.150	0.155	0.158	0.153	0.153	0.942	0.932	0.945	0.943

Table 2: MSE two datasets without locations as sources.

Model	MSE				Small MSE			
	Reg	Tree	RF	BART	Reg	Tree	RF	BART
<i>Dissecting Bias Health</i>								
JTT	0.167	0.229	0.200	0.196	0.141	0.187	0.173	0.174
RWG	0.167	0.178	0.166	0.165	0.141	0.158	0.142	0.139
Global	0.167	0.173	0.166	0.166	0.141	0.162	0.142	0.143
Local	0.171	0.193	0.172	0.167	0.158	0.159	0.147	0.147
TRL	0.167	0.170	0.165	0.165	0.142	0.159	0.140	0.143
CTRL	0.167	0.169	0.165	0.165	0.141	0.158	0.140	0.144
<i>UK Asylum Decisions</i>								
JTT	0.190	0.243	0.219	0.201	0.149	0.237	0.185	0.154
RWG	0.187	0.193	0.192	0.184	0.138	0.149	0.149	0.138
Global	0.187	0.194	0.192	0.183	0.136	0.150	0.149	0.139
Local	0.200	0.196	0.189	0.186	0.164	0.145	0.134	0.137
TRL	0.186	0.189	0.191	0.182	0.136	0.138	0.134	0.132
CTRL	0.186	0.188	0.190	0.181	0.136	0.139	0.132	0.132

datasets for all available evaluation metrics for those datasets. CTRL shows the best rank across all datasets and metrics. Additional aggregated results are in the appendix.

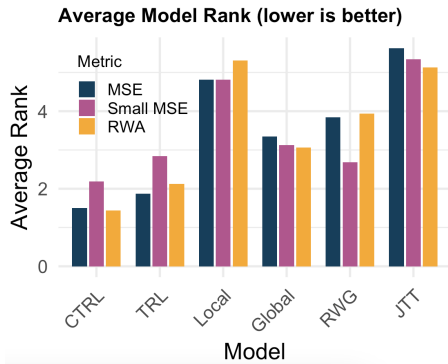


Figure 2: Average model performance ranks across datasets.

Discussion and Conclusion

In the presence of distribution shift across many datasets of varying sizes, standard transfer learning approaches such as cross-domain residual learning can struggle due to uneven

sample sizes and variable feature distributions. We propose a meta-learning algorithm, CTRL, that strikes a balance between leveraging the richness of the full dataset and learning location-specific heterogeneity. More specifically, CTRL combines residual learning with dataset-adaptive pooling to improve predictive performance and reliability in the many-dataset setting.

CTRL is adaptive in that it learns shared predictive structure between locations without requiring prior knowledge of dataset similarity. This is especially valuable in applied contexts where similarities may arise from latent or unobserved factors—such as administrative systems or economic patterns—and are difficult to encode directly. Additionally, CTRL is model-agnostic, making it a strong candidate for deployment in practical settings where interpretability, computational cost, and complexity must be carefully balanced.

That said, our current approach has limitations that merit discussion. First, while the runtime was reasonable for our applications (e.g., 3 hours on an 8-core machine for a dataset of 25,000 observations), it might be prohibitive in other settings. Furthermore, CTRL addresses random shifts in X and conditional $Y|X$ distributions, but it may not be appropriate for settings involving adversarial shifts between locations.

To conclude, our work is motivated by a high-impact, real-world problem: the geographic assignment of asylum seekers in Switzerland. We show that CTRL not only maintains strong accuracy but also improves a key ranking metric, which is particularly relevant for informing downstream tasks.⁷ To support further research and adaptation, we release our codebase along with adapted versions of four out of five datasets⁸: <https://anonymous.4open.science/r/CtrlYourShift-258B/>.

⁷We aim to provide predictions that support—not replace—the work of our partners making critical downstream decisions. Any output from our model must be interpreted and finalized through the lens of stakeholder expertise.

⁸The Swiss Asylum Seekers dataset is not publicly available, but can be requested from the Swiss State Secretariat for Migration.

Acknowledgements

The authors are grateful to the Swiss State Secretariat for Migration (SEM) for providing access to the data and offering valuable guidance. The Swiss asylum data used in this study were made available through a collaborative research agreement with SEM, which prohibits the transfer or disclosure of these data. The authors also thank the GeoMatch team and the Stanford Immigration Policy Lab for their invaluable feedback throughout the development of this project. Rothenhäusler gratefully acknowledges support as a David Huntington Faculty Scholar, Chamber Fellow, and from the Dieter Schwarz Foundation.

References

- Ahani, N.; Gözl, P.; Procaccia, A. D.; Teytelboym, A.; and Trapp, A. C. 2021. Dynamic Placement in Refugee Resettlement. In *Proceedings of the 22nd ACM Conference on Economics and Computation*, EC '21, 5–5. ACM.
- Bansak, K.; and Paulson, E. 2024. Outcome-Driven Dynamic Refugee Assignment with Allocation Balancing. *Operations Research*, 72(6): 2263–2775.
- Bansak, K. C.; Paulson, E.; and Rothenhäusler, D. 2024. Learning under random distributional shifts. In *International Conference on Artificial Intelligence and Statistics*, 3943–3951. PMLR.
- Bowyer, K. W.; Chawla, N. V.; Hall, L. O.; and Kegelmeyer, W. P. 2011. SMOTE: Synthetic Minority Over-sampling Technique. *CoRR*, abs/1106.1813.
- Demšar, J. 2006. Statistical Comparisons of Classifiers over Multiple Data Sets. *J. Mach. Learn. Res.*, 7: 1–30.
- Ding, F.; Hardt, M.; Miller, J.; and Schmidt, L. 2021. Retiring Adult: New Datasets for Fair Machine Learning. *Advances in Neural Information Processing Systems*, 34.
- Fan, J.; and Alvarez-Melis, D. 2023. Generating Synthetic Datasets by Interpolating along Generalized Geodesics. arXiv:2306.06866.
- Friedman, J. H. 2001. Greedy function approximation: a gradient boosting machine. *Annals of statistics*, 1189–1232.
- Hastie, T.; Tibshirani, R.; Friedman, J.; and Franklin, J. 2004. The Elements of Statistical Learning: Data Mining, Inference, and Prediction. *Math. Intell.*, 27: 83–85.
- Huang, C.; and Wang, K. 2025. A Stability Principle for Learning Under Nonstationarity. *Operations Research*.
- Idrissi, B. Y.; Arjovsky, M.; Pezeshki, M.; and Lopez-Paz, D. 2022. Simple data balancing achieves competitive worst-group-accuracy. arXiv:2110.14503.
- Jeong, Y.; and Rothenhäusler, D. 2024. Out-of-distribution generalization under random, dense distributional shifts. *arXiv preprint arXiv:2404.18370*.
- Jeong, Y.; and Rothenhäusler, D. 2025. Out-of-distribution generalization under random, dense distributional shifts. arXiv:2404.18370.
- Khan, F.; and Bremond, F. 2019. Cross domain residual transfer learning for person re-identification. In *2019 IEEE Winter Conference on Applications of Computer Vision (WACV)*. IEEE.
- Künzel, S. R.; Sekhon, J. S.; Bickel, P. J.; and Yu, B. 2019. Metalearners for estimating heterogeneous treatment effects using machine learning. *Proceedings of the National Academy of Sciences*, 116(10): 4156–4165.
- Liu, E. Z.; Haghighi, B.; Chen, A. S.; Raghunathan, A.; Koh, P. W.; Sagawa, S.; Liang, P.; and Finn, C. 2021. Just Train Twice: Improving Group Robustness without Training Group Information. arXiv:2107.09044.
- Liu, J.; Wang, T.; Cui, P.; and Namkoong, H. 2023. On the Need for a Language Describing Distribution Shifts: Illustrations on Tabular Datasets. In Oh, A.; Naumann, T.; Globerson, A.; Saenko, K.; Hardt, M.; and Levine, S., eds., *Advances in Neural Information Processing Systems*, volume 36, 51371–51408. Curran Associates, Inc.
- Long, M.; Zhu, H.; Wang, J.; and Jordan, M. I. 2016. Unsupervised domain adaptation with residual transfer networks. *Advances in neural information processing systems*, 29.
- Meinshausen, N.; and Bühlmann, P. 2010. Stability selection. *Journal of the Royal Statistical Society Series B: Statistical Methodology*, 72(4): 417–473.
- Nie, X.; and Wager, S. 2020. Quasi-Oracle Estimation of Heterogeneous Treatment Effects. arXiv:1712.04912.
- Obermeyer, Z.; Powers, B.; Vogeli, C.; and Mullainathan, S. 2019. Dissecting racial bias in an algorithm used to manage the health of populations. *Science*, 366(6464): 447–453.
- Rudin, C. 2019. Stop Explaining Black Box Machine Learning Models for High Stakes Decisions and Use Interpretable Models Instead. arXiv:1811.10154.
- Sagawa, S.; Koh, P. W.; Hashimoto, T. B.; and Liang, P. 2020. Distributionally Robust Neural Networks for Group Shifts: On the Importance of Regularization for Worst-Case Generalization. arXiv:1911.08731.
- Shen, J. H.; Raji, I. D.; and Chen, I. Y. 2024. The Data Addition Dilemma. In *Proceedings of the 9th Machine Learning for Healthcare Conference*, volume 252 of *Proceedings of Machine Learning Research*. PMLR.
- Wolpert, D. H. 1992. Stacked generalization. *Neural networks*, 5(2): 241–259.
- Xie, S. M.; Pham, H.; Dong, X.; Du, N.; Liu, H.; Lu, Y.; Liang, P.; Le, Q. V.; Ma, T.; and Yu, A. W. 2023. DoReMi: Optimizing Data Mixtures Speeds Up Language Model Pre-training. ArXiv:2305.10429.
- Yadlowsky, S.; Fleming, S.; Shah, N.; Brunskill, E.; and Wager, S. 2025. Evaluating Treatment Prioritization Rules via Rank-Weighted Average Treatment Effects. *Journal of the American Statistical Association*, 120(549): 38–51. PMID: 40248684.
- Ye, J.; Liu, P.; Sun, T.; Zhou, Y.; Zhan, J.; and Qiu, X. 2024. Data Mixing Laws: Optimizing Data Mixtures by Predicting Language Modeling Performance. ArXiv:2403.16952.
- Yosinski, J.; Clune, J.; Bengio, Y.; and Lipson, H. 2014. How transferable are features in deep neural networks? *Advances in neural information processing systems*, 27.

Zhang, H.; Cisse, M.; Dauphin, Y. N.; and Lopez-Paz, D. 2018. mixup: Beyond Empirical Risk Minimization. arXiv:1710.09412.

Zhang, I.; and Rothenhäusler, D. 2025. Data quality or data quantity? Prioritizing data collection under distribution shift with the data usefulness coefficient. *arXiv preprint*. Preprint.

Zhang, Y.; Huang, M.; and Imai, K. 2024. Minimax Regret Estimation for Generalizing Heterogeneous Treatment Effects with Multisite Data. arXiv:2412.11136.

Appendix

Proof of Proposition 1

Proof. For $X \in L$ we can decompose

$$\begin{aligned} R^g &= Y - \hat{E}_{\text{pooled}}[Y | X \in L] \\ &= (Y - E_g[Y | X \in L]) + (E_g[Y | X \in L] \\ &\quad - \hat{E}_{\text{pooled}}[Y | X \in L]), \end{aligned}$$

where \hat{E}_{pooled} denotes the empirical mean over the pooled data. Furthermore, for $X \in L$,

$$r_m = \hat{E}_m[Y|X \in L] - \hat{E}_{\text{pooled}}[Y|X \in L]$$

Now, leveraging the CLT in Zhang and Rothenhäusler (2025), we can use a Taylor expansion

$$\begin{aligned} &E_g[Y|X \in L] - \hat{E}_{\text{pooled}}[Y|X \in L] \\ &= \frac{E_g[Y \cdot 1_{X \in L}]}{E_g[1_{X \in L}]} - \frac{\hat{E}_{\text{pooled}}[Y \cdot 1_{X \in L}]}{\hat{E}_{\text{pooled}}[1_{X \in L}]} \\ &= \frac{E_g[Y \cdot 1_{X \in L}] - \hat{E}_{\text{pooled}}[Y \cdot 1_{X \in L}]}{E_g[1_{X \in L}]} \\ &\quad - \frac{(E_g[1_{X \in L}] - \hat{E}_{\text{pooled}}[1_{X \in L}]) \cdot E_g[Y \cdot 1_{X \in L}]}{E_g[1_{X \in L}]^2} \\ &\quad + o_P(K^{-1/2}) \\ &= (E_g[\phi_L] - \hat{E}_{\text{pooled}}[\phi_L]) + o_P(K^{-1/2}) \end{aligned}$$

Here, $\phi_L = \frac{1_{X \in L}}{P_g(X \in L)}(Y - E_g[Y|X \in L])$.

Analogously, for $X \in L$,

$$r_m = \hat{E}_m[\phi_L] - \hat{E}_{\text{pooled}}[\phi_L] + o_P(K^{-1/2}).$$

Thus,

$\mathcal{E}_g(\mathcal{C})$

$$\begin{aligned} &= \sum_{L \in \mathcal{L}} P_g(X \in L) \cdot (E_g[Y|X \in L] - \hat{E}_{\text{pooled}}[Y|X \in L] \\ &\quad - \sum_{m=1}^{|\mathcal{M}|} \frac{z_m n_m}{\sum_{m'} n_{m'} z_{m'}} (\hat{E}_m[Y|X \in L] - \hat{E}_{\text{pooled}}[Y|X \in L]))^2 \\ &= \sum_{L \in \mathcal{L}} P_g(X \in L) \cdot (E_g[\phi_L] - \hat{E}_{\text{pooled}}[\phi_L] \\ &\quad - \sum_{m=1}^M \frac{z_m n_m}{\sum_{m'} n_{m'} z_{m'}} \cdot (\hat{E}_m[\phi_L] - \hat{E}_{\text{pooled}}[\phi_L]))^2 \\ &= \sum_{L \in \mathcal{L}} P_g(X \in L) \cdot (E_g[\phi_L] - \sum_{m=1}^{|\mathcal{M}|} \frac{z_m n_m}{\sum_{m'} n_{m'} z_{m'}} \cdot \hat{E}_m[\phi_L])^2 \\ &\quad + o_P(K^{-1/2}) \end{aligned}$$

Now we can use a distributional CLT from (Zhang and Rothenhäusler 2025) to obtain that the vector

$$\left(\sqrt{K} \left(E_g[\phi_L] - \sum_{m=1}^{|\mathcal{M}|} \frac{z_m n_m}{\sum_{m'} n_{m'} z_{m'}} \hat{E}_m[\phi_L] \right) \right)_{L \in \mathcal{L}}$$

converge jointly (jointly across $L \in \mathcal{L}$) to a Gaussian random vector with componentwise variance

$$(\beta(\mathcal{C})^\top \Sigma^W \beta(\mathcal{C}) + \sum_m \beta_m^2(\mathcal{C}) c_m) \text{Var}_g(\phi_L).$$

Thus,

$$\begin{aligned} &K \left(E_g[\phi_L] - \sum_{m=1}^{|\mathcal{M}|} \frac{z_m n_m}{\sum_{m'} n_{m'} z_{m'}} \hat{E}_m[\phi_L] \right)^2 \\ &\xrightarrow{d} \chi_1^2 \left((\beta(\mathcal{C})^\top \Sigma^W \beta(\mathcal{C}) + \sum_m \beta_m^2(\mathcal{C}) c_m) \text{Var}_g(\phi_L) \right) \end{aligned}$$

Hence,

$$K \sum_{L \in \mathcal{L}} P_g(X \in L) \left(E_g[\phi_L] - \sum_{m=1}^{|\mathcal{M}|} \frac{z_m n_m}{\sum_{m'} n_{m'} z_{m'}} \hat{E}_m[\phi_L] \right)^2$$

converges to a random variable with mean

$$\sum_{L \in \mathcal{L}} P_g(X \in L) (\beta(\mathcal{C})^\top \Sigma^W \beta(\mathcal{C}) + \sum_m \beta_m^2(\mathcal{C}) c_m) \text{Var}_g(\phi_L).$$

Using that $P_g(X \in L) \text{Var}_g(\phi_L) = \text{Var}_g(Y|X \in L)$, we can rewrite the previous display as

$$\sum_{L \in \mathcal{L}} (\beta(\mathcal{C})^\top \Sigma^W \beta(\mathcal{C}) + \sum_m \beta_m^2(\mathcal{C}) c_m) \text{Var}_g(Y|X \in L).$$

This completes the proof. \square

RWA across different thresholds

In the main paper, we report RWA results using the top 20% of individuals per location. This threshold provides a practical balance: it captures meaningful location-specific variation in predicted outcomes while avoiding the inclusion of too many individuals, which could obscure differences by averaging them out. To examine the sensitivity of our findings to this choice, we also report RWA results for a range of threshold levels in Table 3. Across all thresholds, CTRL consistently performs better than the comparison methods.

At the 10% threshold, the Global and JTT models perform comparatively well on the Education dataset. This is not unexpected, as the top 10% of individuals are likely those who would achieve good outcomes in most locations, making globally optimized models like Global and JTT more effective in this narrow slice. Even in this case, CTRL performs similarly, highlighting its effectiveness across different evaluation settings. Lastly, these results are shown only for datasets that involve an explicit decision-making task: the synthetic dataset, the Swiss Asylum Seekers dataset, and the Education dataset.

Table 3: Average RWA across different top percentages for all datasets. Bold indicates best performance within each dataset and column.

Model	Top 10%				Top 20%				Top 30%				Top 40%				Top 50%			
	Reg	Tree	RF	BART	Reg	Tree	RF	BART	Reg	Tree	RF	BART	Reg	Tree	RF	BART	Reg	Tree	RF	BART
Synthetic Dataset																				
JTT	0.820	0.616	0.822	0.832	0.789	0.604	0.784	0.798	0.747	0.586	0.749	0.760	0.712	0.575	0.707	0.720	0.674	0.573	0.672	0.679
RWG	0.820	0.669	0.805	0.814	0.789	0.669	0.759	0.778	0.747	0.669	0.725	0.738	0.712	0.656	0.691	0.697	0.674	0.639	0.660	0.663
Local	0.962	0.649	0.930	0.951	0.930	0.661	0.884	0.907	0.890	0.659	0.838	0.860	0.842	0.649	0.791	0.811	0.788	0.628	0.743	0.760
Global	0.776	0.694	0.765	0.808	0.744	0.686	0.732	0.769	0.714	0.665	0.702	0.734	0.683	0.646	0.673	0.700	0.653	0.624	0.644	0.667
TRL	0.964	0.746	0.908	0.952	0.934	0.726	0.863	0.911	0.895	0.696	0.820	0.865	0.847	0.668	0.776	0.816	0.791	0.640	0.731	0.764
CTRL	0.983	0.776	0.937	0.970	0.957	0.745	0.895	0.933	0.920	0.715	0.852	0.888	0.872	0.687	0.805	0.838	0.813	0.658	0.756	0.783
Swiss Asylum Seekers Dataset																				
JTT	0.408	0.345	0.327	0.293	0.264	0.245	0.243	0.251	0.254	0.252	0.504	0.420	0.369	0.320	0.291	0.502	0.406	0.347	0.314	0.281
RWG	0.445	0.363	0.337	0.298	0.270	0.371	0.342	0.309	0.280	0.246	0.494	0.412	0.359	0.318	0.289	0.514	0.404	0.350	0.315	0.281
Global	0.448	0.356	0.339	0.301	0.269	0.484	0.376	0.338	0.303	0.268	0.512	0.410	0.362	0.330	0.292	0.510	0.403	0.352	0.315	0.281
Local	0.422	0.358	0.319	0.294	0.267	0.370	0.307	0.284	0.263	0.248	0.488	0.398	0.348	0.314	0.285	0.457	0.368	0.331	0.303	0.273
TRL	0.457	0.373	0.338	0.304	0.272	0.486	0.377	0.333	0.302	0.268	0.512	0.422	0.360	0.328	0.294	0.516	0.414	0.357	0.319	0.281
CTRL	0.466	0.375	0.341	0.308	0.274	0.484	0.390	0.341	0.304	0.274	0.525	0.420	0.363	0.328	0.297	0.512	0.414	0.354	0.316	0.284
Education Dataset																				
JTT	0.953	0.916	0.927	0.964	0.936	0.894	0.908	0.944	0.917	0.862	0.893	0.926	0.901	0.854	0.876	0.907	0.886	0.843	0.855	0.890
RWG	0.953	0.927	0.961	0.954	0.937	0.919	0.940	0.940	0.918	0.906	0.919	0.917	0.902	0.878	0.901	0.897	0.886	0.869	0.887	0.886
Global	0.953	0.925	0.964	0.960	0.940	0.913	0.942	0.943	0.918	0.909	0.926	0.924	0.902	0.881	0.909	0.906	0.887	0.869	0.890	0.889
Local	0.871	0.873	0.944	0.952	0.898	0.880	0.932	0.940	0.899	0.876	0.915	0.927	0.889	0.851	0.897	0.908	0.873	0.838	0.883	0.893
TRL	0.952	0.941	0.962	0.953	0.941	0.927	0.944	0.943	0.926	0.918	0.929	0.929	0.905	0.892	0.909	0.911	0.889	0.874	0.891	0.893
CTRL	0.950	0.941	0.963	0.954	0.942	0.932	0.945	0.943	0.929	0.920	0.929	0.931	0.907	0.900	0.909	0.912	0.891	0.879	0.891	0.893

Datasets

We make four of the five datasets used in this paper available through our codebase: <https://anonymous.4open.science/r/CtrlYourShift-258B/>, along with a README containing instructions for accessing all datasets. Table 4 also provides a detailed overview of each dataset, including information on features, outcomes, source structure, and sample size. The full Education, Dissecting Bias in Health, and UK Asylum Decisions datasets are publicly accessible, and links to their original sources can be found in the paper’s citations and the codebase README. We additionally provide adapted versions of the datasets that reflect a multi-source structure, where each source has a unique relationship between its features and outcome variable. We hope this can help facilitate further research on prediction tasks for datasets with imbalanced and heterogeneous sources.

We selected these datasets to reflect both our real-world motivation and broader methodological relevance. The Swiss Asylum Seekers dataset directly motivated the development of CTRL, as this work emerged from a real-world collaboration focused on improving decision-making for asylum seeker placement in Switzerland, where data sparsity and heterogeneity across locations present significant challenges. The Education data is an adapted version of United States Census data for which we turn to Ding et al. (2021) for pre-processing. This dataset is commonly used for studying debiasing, fairness, and distribution shift, making it a natural testbed for us (Liu et al. 2023; Jeong and Rothenhäusler 2024). The Dissecting Bias in Health datasets was similarly constructed for this sort of analysis (Obermeyer et al. 2019). Finally, we introduce the UK Asylum Decisions dataset, which, to the best of our knowledge, has not been used in prior machine learning research. However, it naturally exhibits both distribution shift and many-source structure, making it a promising and relevant benchmark for researchers interested in studying these challenges and exploring new real-world datasets. Its inclusion supports a more concrete observation: although CTRL was originally developed with a specific ap-

plication in mind, many real-world datasets naturally take the form of imbalanced, unevenly sized many-source settings. This paper takes a step toward developing practical tools that are explicitly designed to handle such structure

Due to privacy constraints, we are unable to release the Swiss Asylum Seekers dataset, as it contains sensitive, non-public information.

Synthetic Data Generation

To evaluate CTRL in a more controlled setting, we construct a synthetic dataset designed to reflect the key challenge CTRL aims to address: learning accurate, location-specific predictions when data availability is highly uneven across sources. We generate $N = 40,000$ individual observations assigned to $|\mathcal{M}| = 50$ locations, each denoted by $g \in \mathcal{M}$, with a minimum location size of 120 and the max around 3000. Location sizes are drawn from a Pareto distribution to simulate naturally imbalanced settings.

Each individual is assigned a $d = 20$ -dimensional feature vector drawn from a standard normal distribution. Outcome probabilities are computed as a weighted combination of global and location-specific signal components, passed through a sigmoid to map values to $[0, 1]$, with binary outcomes sampled accordingly. A subset of locations are grouped into latent clusters of size 2–7, where each location g shares a common base weight vector with small random shifts. The remaining locations are assigned weights independently, with each location having its own feature-level means and variances. For the experiments in this paper, we use a weighting of 0.3 on the global signal and 0.7 on the local (location-specific) signal when combining probabilities. We selected this ratio based on empirical observations that our baseline TRL achieved greater performance gains under this structure, suggesting that this weighting provides a favorable balance between pooled information and location-specific variation. It reflects a setting where shared signal is informative but insufficient on its own, requiring local adaptation to fully capture heterogeneous outcome patterns.

Table 4: Overview of datasets used in our experiments.

Title	Outcome	Sources	Source Info	Overall Size	Train Size	Test Size	Features
Synthetic	simulated outcome	simulated distributional shifts	50 sources (sizes 40-2000)	40,000	13,320	26,680	20 random continuous features
Swiss Asylum	binary two year employment outcome	cantons	26 cantons (sizes 50-3900)	~30,000	~24,000	~6000	135 continuous or one hot encoded variabes - demographics, language, arrival time, administrative info, etc.
Education	binary high school graduate status	US states (including PR)	51 states/territories (sizes 244-122092)	470,442	94,089	376,353	13 one hot encoded variables - demographic, ethnicity, citizenship, language, disability
UK Asylum Decisions	binary asylum approval outcome	nationality	103 nationalities (sizes 41-1918)	84,449	42,225	42,224	108 one hot encoded and continuous variables features - demographics, administrative info, arrival time
Dissecting Health Bias	binary indicator of chronic illness	race+gender+age demographic group (e.g. "18-24_0_black" is a group for age 18-24 men that are black)	28 groups (sizes 76-6453)	47,865	28,719	19,146	93 one hot encoded and continuous variables - risk score, health indicators, enrolled program

While this dataset is constructed to represent the types of structure CTRL is designed to handle—namely, latent similarity across some locations—it is important to note that the data is not generated using the CTRL algorithm, nor does it rely on residual modeling. In fact, there is no explicit notion of residuals in the data-generating process. Because each location’s outcome is generated using a linear transformation of features, the true model for each group g is just a linear regression. This remains true even when combining pooled and location-specific components—since the weighted sum of linear functions is itself linear. Therefore, with sufficient data per location, location-level linear models would be the optimal choice. This is reflected in our empirical results (Table 1), where local linear model did actually perform best in overall MSE. However, in small-sample regimes (as shown in Table 1), local models degrade rapidly, and CTRL’s advantage becomes clear. By adaptively pooling data based on similarity across locations, CTRL is able to improve prediction performance—even in cases where the data was not explicitly generated to include residual-based or hierarchical structure—demonstrating its adaptability to realistic many-source (or *many-location*) settings.

We include the generated dataset and the full script used to construct it, ‘generate_synthetic_data.py’, in our codebase. The script allows users to easily reproduce or modify the synthetic data for further experimentation.

Overall Performance

Evaluating CTRL across multiple datasets is essential for assessing its robustness and broader applicability. In addition to dataset-specific analyses, we summarize CTRL’s average performance across all datasets to provide a more holistic

view. Figure 2 presents an average rank metric, while Figure 3 displays the average performance gap between CTRL and each benchmark method. We exclude the synthetic dataset from this comparison, as it was explicitly constructed to align with our modeling assumptions.

In Figure 3, positive values indicate that a benchmark performs worse than CTRL. Across all evaluation metrics—MSE, Small MSE, and RWA—all benchmarks underperform relative to CTRL on average. The improvement in the RWA metric is particularly noteworthy, as it directly reflects the model’s ability to rank people at different locations effectively. Given our goal of improving decision-making for asylum seeker placement in Switzerland, this result highlights CTRL’s potential to inform real-world allocation policies.

Combinatorial Optimization

In order to solve Problem 1 we need to utilize the NonConvex solver with Gurobi. Additionally, running it for all groups ends up becoming extremely slow, so we use a random subset of 5-7 groups for every run depending on how large the dataset is (more than this and the optimization problems takes much longer to solve). After repeating 250 times, we can average over all the runs to get an overall location ranking even though each individual run only looks at a subset.

CTRL Parameters

We conduct simulations on synthetic data to guide the selection of optimal hyperparameters for our CTRL framework. For generating the initial weights w_g , we rerun Algorithm 1 250 times. This decision is motivated by empirical observations: after approximately 150 iterations, the average change in the top five source locations (as ranked for each target

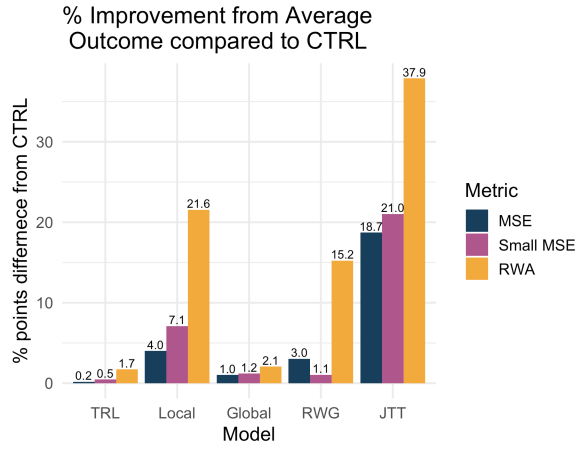


Figure 3: Average performance gaps relative to CTRL are shown across all applicable datasets for each metric, excluding the synthetic dataset, which was specifically constructed for our use case. A positive value here indicates worse performance.

location’s cluster) stabilizes to around 0.25 locations (see Figure 4). This suggests that beyond this point, the top-ranked source locations remain largely consistent. We use the average change in the top 5 as our stability metric because cluster sizes tend to average around five (see Figure 7 for cluster examples), making it more critical to identify the correct set of source locations than to determine their exact order within the ranking. Thus, our metric prioritizes inclusion over position.

For estimating the mean squared error (MSE) in Algorithm 2, we also select 250 iterations. As shown in Figure 5, the L1 change in consecutive \mathbf{k}^* s—the vector of optimal top- k values (k_ℓ^*) across all target locations—decreases and converges to under 5 after approximately 50 iterations. Given that there are 50 target locations in the synthetic dataset, this implies that the expected change in k_ℓ^* for a given location with each additional iteration is about 0.1. Therefore, we consider any iteration count beyond 50 to yield stable and reliable results, and choose 250 to match the splits we use for the \mathbf{w}_g generation.

We constrain the value of k in Algorithm 2 to be at most 10. Empirically, we observe that beyond this threshold, the selected clusters begin to resemble those from a global model, diminishing the benefits of location-specific modeling. Therefore, to preserve the uniqueness of each target location, we limit the number of source locations considered for its cluster to 10. Figure 6 illustrates this trend using the state of Alaska from the education dataset: the MSE plateaus after only five source locations are included, a pattern that holds across most target locations. Nonetheless, we allow k to reach up to 10 to provide some buffer. In practice, we find that most location clusters are around or less than 5 source locations. For reference, all generated clusters for the education dataset are visualized in Figure 7.

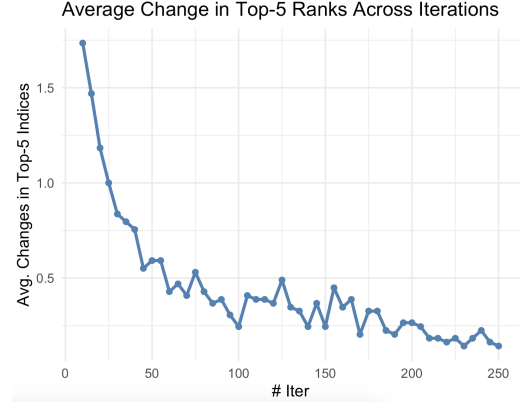


Figure 4: Change in top 5 locations picked as we add more iterations for running Algorithm 1. We reach about 0.25 changes per location after 150 iterations.

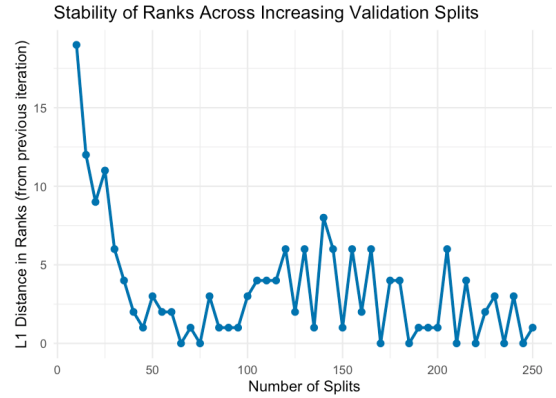


Figure 5: Change in ranks vector \mathbf{k}^* returned by Algorithm 2 for all locations $g \in \mathcal{M}$. L1 distance between \mathbf{k}^* and $\mathbf{k}^{*(+5)}$ corresponding to the i ’th and $i + 5$ ’th validation split.

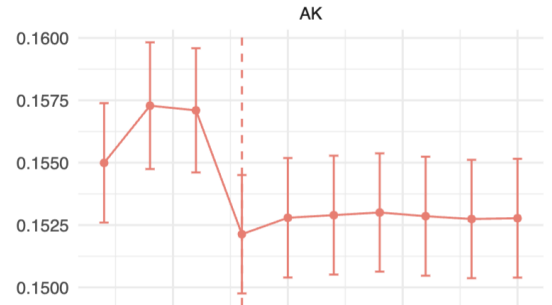


Figure 6: Change in cross validated MSE as we add more source locations to train $\hat{f}_{\text{residual}}^{\mathcal{C}(g)}$ for the state of Alaska. The dotted line represents the actual k^* picked for Alaska.

State Groups - Target to Sources Table

Target	Sources	Target	Sources
AK	HI, MT, NC	MT	SD
AL	ID	NC	AL, MI, GA
AZ	GA, PA, CO, NM, DE, LA, MO, MS, TX	ND	MT
CO	NC, GA, AR, NV	NE	AR
CT	LA	NH	LA
DE	AR, AL, MT	NJ	VT, SD, RI, HI, MA
FL	VT, LA, MT	NV	ID, AR
GA	NC, NE	OK	ID
IA	AR, NV, IN, ID	OR	ID, AR, CA
ID	DE, CA	PA	MT, IN, OH
IN	AR, OH	RI	HI, KS, NJ
KS	MT, NV	SC	NC, AR, NV, TX
KY	IN	SD	MT
LA	VT, MT	TN	ID, OH, AR
MD	CA	VA	NC
ME	VT, LA	VT	MT, LA
MI	OH, WY	WA	NV, AR, ID, NE, CA
MN	SD, MT, OK, VT, PA, HI	WI	MT, SD, IN, OH
MO	IN, SD, MT, OH	WV	CO

Figure 7: Table showing the source clusters created by CTRL for each target state in the Education datasets. We omit states that only picked themselves for their cluster. Every state is required to pick itself as a source (see Equation 1), but we don't explicitly write that in the table for simplicity.